A review on heat transfer and hydrodynamic characteristics of nano/microencapsulated phase change slurry (N/MPCS) in mini/microchannel heat sinks

Lei Chai[a,b *], Rabia Shaukat[a,c], Liang Wang[d], Hua Sheng Wang[a]

[a] School of Engineering and Materials Science, Queen Mary University of London, Mile End Road, London E1 4NS, UK

[b] RCUK National Centre for Sustainable Energy Use in Food Chain (CSEF), Brunel University London, Uxbridge, Middlesex UB8 3PH, UK

[c] Department of Mechanical Engineering, University of Engineering and Technology, Lahore, Pakista

[d] Institute of Engineering Thermophysics, Chinese Academy of Sciences, Beijing 100190, China

Abstract Mini/microchannel heat sinks are currently widely used in a variety of thermal and energy applications with the advantages of compactness, light weight and higher heat transfer performance. In order to further improve the performance of such heat sink, many recent studies have introduced the nano/microencapsulated phase change slurry (N/MPCS) as the working fluid due to their high storage capacity during phase change. This paper concerns the channel with hydraulic diameter from 10 μm to 3 mm, covering the range of microchannel and minichannel. Firstly, the existed review works relate to mini/microchannel heat sinks are summarized, with topics covering manufacturing processes and geometric designs, thermal and hydrodynamic performance with different working fluids, and their typical and potential applications. Then, the N/MPCS used in mini/microchannels from experimental and numerical simulation works are discussed, with focuses placed on the base fluid, core and shell materials, and thermophysical properties of slurry. Next, the local, average and overall heat transfer and hydrodynamic characteristics of mini/microchannel heat sinks with N/MPCS flowing inside are reviewed and analyzed, considering different flow conditions, material and dimension of test section, and composition and fraction of such slurry. Finally, the proposed heat transfer and pressure drop correlations in this research field are evaluated. The purpose of this review article is to provide exhaustive and comprehensive study of recent published works in this new area and supply useful

* Corresponding author. Tel.: +44 (0)1895 265834.

E-mail address: l.chai@outlook.com (Lei Chai).

information for the design of compact heat exchangers and thermal storage systems with N/MPCS as working fluid.

Key words Mini/microchannel heat sink; nano/microencapsulated phase change slurry; heat transfer and hydrodynamic characteristics

Contents

1. Introduction

Mini/microchannel heat sinks as shown in Fig. 1 (arbitrarily defined here as channels with a hydraulic diameter from 10 μm to 3 mm as Kandlikar and Grande [1]) are currently widely used for the high heat flux applications such as electronics cooling, due to their advantages of compactness, light weight and higher heat transfer surface area to fluid volume ratio compared with other macroscale

systems [2]. More recently, the necessity to further miniaturize the advanced computational instruments and remove the higher heat generated by these microprocessors, requires more innovative ideas in design of mini/micro cooling systems.

In order to further enhance the cooling ability of the currently available mini/microchannel heat sinks, researchers have investigated the cooling system configuration [3, 4, 5], working fluids [6, 7, 8] and other relevant parameters [9-12]. Among these methods, the mini/microchannel heat sink with N/MPCS as working fluid has attracted the researchers' attentions, because it combines the advantages of both mini/microchannel and N/MPCS. The N/MPCS is a liquid in which phase change material (PCM) is encapsulated in a nano/microcapsule and is dispersed in base fluid. Compared to base fluid, the N/MPCS has a higher apparent heat capacity during phase change and almost constant temperature during charging and discharging processes. Further, the nano/microencapsulation can increase the heat transfer area and thermal conductivity speed of phase change slurry (PCS), and the nano/microsized shell can prevent PCM from fusion and agglomeration, to increase the stability of particles inside [13, 14].

In recent years, new frontiers have been opened up for mini/microchannel heat sinks design and applications. Microchannel heat sinks incorporating single-phase liquid flow, as an efficient means to meet the demand of high heat removal, are used in a variety of devices. Several review papers have also been published in this area to present the status of the art [15-20], but very little review papers focus on the N/MPCS in mini/microchannel heat sinks, although some experimental, numerical and analytical model works have been conducted in this area. Further, most of the N/MPCS review articles [21-29] concern the thermophysical properties, manufacturing methods and applications. Until now, the mini/microchannel heat sinks combining with N/MPCS have not effectively incorporated into real applications, thus more research efforts are needed. This paper comprehensively reviews current researches of mini/microchannel heat sinks with N/MPCS as working fluid. Based on the summary and analysis of major experimental and numerical results, the thermal and hydrodynamic properties for such heat sinks are made in this study.

2. Mini/microchannel heat sink

The concept of mini/microchannel heat sink was firstly proposed by Tuckerman and Pease [30] in 1981. Since then, many authors have performed studies on the thermal and hydrodynamic performance of mini/microchannel heat sinks in dissipating high heat flux. In contrast to traditional tube heat exchangers, mini/microchannel heat sinks can result in much higher heat transfer performance and significantly reduced weight for a given heat duty, making them more suitable for applications with energy requirements, space limitations, and materials savings. Until now, various review works on mini/microchannel heat sinks or mini/microchannel heat exchangers have been conducted.

The higher volumetric heat transfer densities require advanced manufacturing techniques and more complex manifold designs. Madou [31], Ashman and Kandlikar [32] and Dixit and Ghosh [19] summarized the manufacturing processes being used in the fabrication of mini/microchannel heat sinks and compared the different techniques related to tolerances and material compatibility. Naqiuddin et al. [33] reviewed the different geometric design of mini/microchannels which were derived from numerical simulation and experimental works. Sidik et al. [34] and Dewan and Srivastava [35] comprehensively discussed the passive techniques for heat transfer augmentation in mini/microchannels.

Employing mini/microchannels results in higher heat transfer performance, but is usually accompanied by a higher pressure drop per unit length, making the studies of heat transfer and fluid flow in mini/microchannels are the prerequisites for using them in any thermal applications. Rostami et al. [36] and Agrawal [37] summarized theoretical and experimental works related to the gas flow and heat transfer in mini/microchannels. Dixit and Ghosh [19] and Adham et al. [38] reviewed the thermal and hydrodynamic performance of single phase fluids flowing through mini/microchannel heat sinks and mini/microchannel heat exchangers. Rosa et al. [18] comprehensively discussed the scaling effects (entrance effects, conjugate heat transfer, viscous heating, electric double layer effects, temperature dependent properties, surface roughness, rarefaction and compressibility effects) on thermo-hydraulic characteristics of single phase flow. Thome [39], Cheng et al. [40, 41] and Karayiannis and Mahmoud [42] reviewed the fundamental issues, mechanisms and models of flow boiling in single or multi mini/microchannels. Kim and Mudawar [43, 44] reviewed the databases and predictive methods for

heat transfer in adiabatic, condensing and boiling mini/microchannel flows. Hussien et al. [6] reviewed the thermo-hydraulic characteristics of micro/minichannels using nanofluids as working fluid.

Mini/microchannel heat sinks are increasingly being used in industry to yield compact geometries for heat transfer in a wide variety of applications. Khan and Fartaj [45] surveyed the potential applications of mini/microchannels as heat exchanger components in typical thermal and energy applications. Mudawar [46] presented a detailed discussion on the possible applications of mini/microchannels heat sinks, including water cooled turbine blades, computer data centers, rocket nozzle cooling, fusion reactor blanket cooling, avionics cooling, cooling of satellite electronics, cooling of hybrid vehicle power electronics, and heat exchangers for hydrogen storage systems, etc. Karayiannis and Mahmoud [42] also demonstrated the applications of mini/microchannels heat sinks as cooling components in computers and information technology (CPUs, GPUs, memory cards, data storage devices), cooling high power semiconductor devices (IGBT inverters and switchmode power supplies), cooling laser diode arrays, cooling proton exchange membrane fuel cells and evaporators/condensers in miniature vapour compression refrigerators.

3. Nano/microencapsulated phase change slurry

3.1 Materials

Heat transfer can be enhanced by improving the thermophysical properties of the process fluid, such as addition of phase change particles. Such functional thermal fluid has a high energy density because they use not only the sensible heat capacity of the base fluid, but also the latent heat capacity of the PCM during the phase change process. During choosing the phase change particles, there are several rules that should be followed as suggested by Chen et al. [15] and Jamekhorshid et al. [26]. For the core materials, the phase change temperature range should be narrow and match the designed temperature, and the volume change during phase change process should be low; for the shell materials, the sealing tightness should be good, the materials should be endurable and elastic and can resist high temperature and pumping; for the N/MPCS, the specific heat should be large and the heat transfer performance should be good. Although many studies have tried to cover the major advantages for specific application designs, it is impossible to find a kind of material that can meet all the requirements.

Table 1 shows the representative properties of N/MPCS used in mini/microchannel heat sinks from experimental researches, while those from numerical studies are shown in Table 2. Figs. 2 (a) and (b) show the SEM images of two types of phase change particle, one is microencapsulated and the other is nanoencapsulated. For N/MPCS, the base fluids are commonly water and poly-a-olefin (PAO), the core materials are usually *n*-octadecane and *n*-eicosane, and the shell materials are mainly polymethyl methacrylate (PMMA) and melamine-formaldehyde resinous. For the *n*-octadecane, the size distribution covers the range of 0.1-10 μm, the phase change temperature ranges from 23 ºC to 33 ºC, and the latent heat is about 240 kJ/kg except the studies of Kuravi et al. [49] and Hao and Tao [55]. For the *n*-eicosane, the size distribution covers the range of 1.5-12 μm, the phase change temperature is 35.8-36.4 ºC for melting and 34.0-34.7 ºC for freezing, and the latent heat is 230-247.3 kJ/kg. Until now, as pointed by Chen et al. [15], microencapsulated phase change material (MPCM) has been studied for many years, but the researches on nanoencapsulated one (NPCM) have just started in recent years. For nanoencapsulated phase change slurry (NPCS), Wu et al. [53] described two types of slurries which was made by a colloid method to suspend the PCM into PAO for potential high temperature (150-180 ºC) applications. The core material is tetraethoxysilane, which has the size distribution 150-1000 nm, phase change temperature 155 ºC for melting and 135 ºC for freezing, and the latent heat 38.5 kJ/kg. It is noted that the subcooling of such NPCS is up to 20 K, which can enlarge the temperature range by decreasing the freezing point. Therefore, the NPCM may not be in complete phase change at the end of the tube, which reduces the energy efficiency in heating or cooling applications. Further, as pointed out by Yamagishi et al [64], the effect of subcooling becomes increasingly significant for some core materials when the size of N/MPCM is less than 100 μm. Thus as the N/MPCS is used as heat transfer fluid, the subcooling problem should be paid much attention for some specific applications. Sinha-Ray et al. [54] described a type of NPCS with PCMs (wax or meso-erythritol) encapsulated in carbon nanotubes (CNTs) by a method of self-sustained diffusion at room temperature and atmosphere pressure. These nano-encapsulated wax nanoparticles allowed heat removal over a relatively wide range of temperatures 40-80 °C, and the nano-encapsulated meso-erythritol nanoparticles allowed heat removal in the range of 118-120 °C. The combination of these two PCMs (wax and meso-erythritol) could extend the temperature range of 40-120 °C, when both types of nanoparticles (wax and meso-erythritol

intercalated) would be suspended in the same carrier fluid (an oil). They also suggested that although NPCS has higher heat transfer coefficient than traditional single phase fluid, the subcooling should be reduced by optimizing shell composition and structure.

3.2 Thermophysical properties

Several experimental results have demonstrated the significance of N/MPCS storage capacity, but the high storage capacity during phase change depends on many factors including the kind of PCM, particle concentration, operating temperature, residence time, etc. Therefore, the prediction models of the thermophysical properties of N/MPCS based on experimental evidences are necessary and required. There are several studies have concerned about measuring and computing of the thermophysical properties of N/MPCS and investigated the effects of temperature on them [21, 65-68].

Mass concentration determines whether N/MPCS can be seen as Newtonian fluid or not, which can be substituted by volume fraction as Chen et al. [69]:

$$c_{\mathrm{v}} = \frac{c_{\mathrm{m}}\rho_{\mathrm{b}}}{\rho_{\mathrm{p}}} \tag{1}$$

where the subscripts p and b refer to particle and slurry, respectively; c_{v} and c_{m} represent volume and mass concentrations, respectively.

The N/MPCS density normally uses the two underlying formulas to predict as Pak et al. [70] and Chen et al. [69]:

$$\rho_{\mathrm{b}} = (1-c_{\mathrm{m}})\rho_{\mathrm{f}} + c_{\mathrm{m}}\rho_{\mathrm{p}} \tag{2}$$

$$\frac{1}{\rho_{\mathrm{b}}} = \frac{1-c_{\mathrm{m}}}{\rho_{\mathrm{f}}} + \frac{c_{\mathrm{m}}}{\rho_{\mathrm{p}}} \tag{3}$$

where the subscript f indicates the base fluid. The density of encapsulated particle ρ_{p} can be calculated by

$$\rho_{\mathrm{p}} = \frac{(1+y)\rho_{\mathrm{c}}\rho_{\mathrm{s}}}{\rho_{\mathrm{s}} + y\rho_{\mathrm{c}}} \tag{4}$$

where the subscripts c and s mean the core and shell, respectively; y is the core-shell weight ratio.

State thermal conductivity of N/MPCS are usually determined by Maxwell Model [71] as follows:

$$k_b = k_f \frac{k_p + 2k_f + 2(k_p - k_f)c_v}{k_p + 2k_f - (k_p - k_f)c_v} \tag{5}$$

This model is normally accurate for spherical encapsulated particle, but the accuracy declines with the shape of suspension particle away from spherical. Therefore, Hamilton and Crosser [72] considered this effect and modified the model as

$$k_b = k_f \frac{k_p + (n-1)k_f + (n-1)(k_p - k_f)c_v}{k_p + (n-1)k_f - (k_p - k_f)c_v} \tag{6}$$

where n is the shape factor and varies in the range of 3-3.13, and for spherical suspension particle shape $n = 3$, which mean that this model reduces to the Maxwell model. In the above two equations, k_p is the thermal conductivity of encapsulated particle, which can be calculated as Chen et al. [69]:

$$\frac{1}{k_p d_p} = \frac{1}{k_c d_c} + \frac{d_p - d_c}{k_s d_p d_c} \tag{7}$$

$$\left(\frac{d_c}{d_p}\right)^3 = \frac{\rho_s}{\rho_s + y\rho_c} \tag{8}$$

Further, due to particle-particle, particle-liquid and particle-wall interactions as N/MPCS flows in the channels, the effective thermal conductivity of slurry increases and can be calculated as Zhang et al. [22]:

$$\frac{k_e}{k_b} = 1 + Bc_v Pe_p^m \tag{9}$$

$$B = 3,\ \mathrm{m} = 1.5,\ Pe_p < 0.67$$

$$B = 1.8,\ \mathrm{m} = 0.18,\ 0.67 < Pe_p < 250$$

$$B = 3,\ \mathrm{m} = \frac{1}{11},\ Pe_p > 250$$

The particle Peclet number is defined as

$$Pe_p = \frac{ed_p^2}{\alpha_f} \tag{10}$$

where α_f is the thermal diffusivity, and e is the shear rate magnitude which can be calculated using the following equation

$$e = \left[\frac{1}{2} \sum_i \sum_j \gamma_{ij} \gamma_{ji} \right]^{1/2} \tag{11}$$

where γ is the shear rate. It can be noted that the effective thermal conductivity is strongly dependent on the shear rate and particle size due to the interactions (drag force, lift force, and virtual mass) between the liquid and the particles (Seyf et al. [61]).

Specific heat of N/MPCS is usually obtained by the following formula for liquid/solid solutions [22, 73-77]:

$$c_{\mathrm{p,b}} = (1 - c_{\mathrm{m}}) c_{\mathrm{p,f}} + c_{\mathrm{m}} c_{\mathrm{p,p}} \tag{12}$$

where $c_{\mathrm{p,p}}$ is the specific heat of encapsulated particles. For the process without phase change, $c_{\mathrm{p,p}}$ can be calculated as Chen et al. [69]:

$$c_{\mathrm{p,p}} = \frac{(c_{\mathrm{p,c}} + y c_{\mathrm{p,s}}) \rho_{\mathrm{c}} \rho_{\mathrm{s}}}{(y \rho_{\mathrm{c}} + \rho_{\mathrm{s}}) \rho_{\mathrm{p}}} \tag{13}$$

If the phase change is involved in estimating the heat transfer performance and the latent heat of the encapsulated particle is known, a sine profile or a rectangular profile can be used to model the specific heat of encapsulated particle [61, 63]:

$$c_{\mathrm{p,p}} = c_{\mathrm{p,c}} + \left\{ \frac{\pi}{2} \cdot \left(\frac{h_{\mathrm{sf}}}{T_{\mathrm{mr}}} - c_{\mathrm{p,c}} \right) \cdot \sin \pi \left[\frac{(T - T_1)}{T_{\mathrm{mr}}} \right] \right\} \tag{14}$$

$$c_{\mathrm{p,p}} = c_{\mathrm{p,c}} + \frac{(T - T_1) h_{\mathrm{sf}}}{T_{\mathrm{mr}}} \tag{15}$$

where T_{mr} is the melting range ($T_{\mathrm{mr}} = T_2 - T_1$). T_1 and T_2 are the start and end point of the melting region, respectively. Fig. 3 shows the predicted specific heat profiles of $c_{\mathrm{p,p}}$ and $c_{\mathrm{p,b}}$, according to the DSC thermal analysis data of dried PCM particles in the heating process from Rao et al. [48], where base fluid is water and PCM is *n*-octadecane with latent heat $h_{\mathrm{sf}} = 241$ kJ/kg. Comparison with the DSC thermal analysis results indicates that $c_{\mathrm{p,p}}$ predicted by Eq. (14) is more reasonable, whose profiles show the increase of heat capacity of encapsulated particle starts from solid state at T_1, reached its maximum during the melting process, and then reduces to the heat capacity of liquid encapsulated particle when it reaches T_2, and for temperatures higher or lower than melting range the value of specific heat of particle is equal to $c_{\mathrm{p,c}}$.

The most common models for predicting the effective viscosity of N/MPCS at lower volume concentration (less than around 30%, considered as Newtonian fluid) include:

Einstein model [78]:

$$\mu_b = (1 + 2.5c_v)\mu_f \tag{16}$$

Batchelor correlation [79]:

$$\mu_b = (1 + 2.5c_v + 6.2c_v^2)\mu_f \tag{17}$$

Vand equation [80]:

$$\mu_b = (1 - c_v - Ac_v^2)^{-2.5}\mu_f \tag{18}$$

The parameter A varies in the range of 1.16-4.5 for different materials and sizes [15]. Vand [80] obtained the value A = 1.16 for the glass sphere with diameter of 13 mm. Mulligan et al. [81] got the value A = 3.4 for the slurry with particle of 10-30 μm in diameter. Yamagishi et al. [82] estimated the value A = 3.7 for the microencapsulated *n*-octadecane slurry with an average diameter of 6.3 μm. Wang et al. [83] obtained the value A = 4.45 for the microencapsulated 1-bromohexadecane slurry with volume average diameter of particles 10.112 μm. Fig. 4 shows the profiles of μ_b/μ_f versus c_v using the above mentioned equations. All the predictions show that when the volume fraction is low (c_v<10%), the viscosity is relatively low and the predictions show little difference from those of base fluid, while c_v>10%, the predictions show much larger difference, particularly for Eq. (18), which dramatically rise with increase of c_v. It should be pointed out that most numerical simulation literatures of N/MPCS in mini/microchannels [57-63] calculate the viscosity of the suspension following Eq. (18) with A = 1.16.

4. Heat transfer and hydrodynamic characteristics

4.1 Non-dimensional numbers

Table 3 shows an overview of the non-dimensional numbers relevant to mini/microchannel heat sinks with N/MPCS flowing inside. The researchers usually use Nusselt number to study the heat transfer characteristics, and Reynolds number and friction factor to study the hydrodynamic characteristics. To investigate the heat transfer properties of N/MPCS, Roy and Avanic [84] and Chen

et al. [69] proposed the Stephen number to denote the ratio of the sensible heat to latent heat in the phase change process. To investigate the hydrodynamic properties of N/MPCS owing to the higher viscosity in comparison with base fluid, Rajabifar et al. [62, 63] demonstrated Euler number variation with NPCM concentration at different inlet velocities, and Euler number was defined as a non-dimensional number related to the ratio of pressure drop of the system and squared Reynolds number. Since generally more pumping power is required for higher heat transfer rate, the performance index is widely used to evaluate the heat transfer performance of N/MPCS in mini/microchannel heat sinks with pumping power limitations. To investigate the effect of particle volume concentration, mass flow rate and heat flux on the thermal performance of N/MPCS in mini/microchannel heat sinks, Alquaity et al. [59, 60] also recommended the effectiveness ratio and Merit number to study such properties. The effectiveness ratio is defined as the ratio of heat transfer rate of N/MPCS to that of base fluid for the same temperature rise from inlet to exit of the microchannel, and indicates the increase of heat transfer rate of the N/MPCS in the same temperature rise as that of the base fluid. Merit number relates to the entropy generation rate due to fluid friction and heat transfer caused by the addition of PCM particles and illustrates the ratio of the gain versus input and losses due to the addition of particles.

4.2 Experimental investigations

Few researchers have exquisitely summarized the literatures on heat transfer and hydrodynamic characteristics of N/MPCS in mini/microchannel heat sinks. Table 4 gives the details of this topic covered in experimental investigations in chorological order.

Rao et al. [47, 48] investigated the laminar flow and convective heat transfer characteristics of MPCS flowing through rectangular copper minichannels. For Reynolds number ranging from 200 to 2000, the experimental data for the suspensions with 0 and 5% concentration agreed well with the existing theoretical model for an incompressible, fully developed, laminar Newtonian flow. For the suspensions with mass concentrations higher than 10%, there was an obvious increase in friction factor and pressure drop in comparison with laminar Newtonian flow. The cooling performance of the MPCS strongly depended on the mass flow rate and the MPCM mass concentration as shown in Fig. 5, which demonstrated the results of Nu_b/Nu_f and $\Delta p_b/\Delta p_f$ with different experimental conditions. Kuravi et al.

[49] studied the heat transfer performance of MPCS in a heat sink with 441 microchannels and found that for developing flows, the performance of such slurry depended on various parameters such as base fluid thermal conductivity, channel dimensions, amount of specific heat used and the particle mass concentration. Their studied slurry performance was poor compared to pure water for all the tested flow rates, particularly for the slurry with higher mass concentrations because of large pressure drop across the microchannel. Dammel and Stephan [50] presented the heat transfer characteristics of laminar MPCS flow through rectangular copper minichannels. They also found that such suspensions were only advantageous in a certain range of parameter combinations. To obtain the benefit of the added MPCM particles, the inlet temperature should be slightly below the theoretical melting temperature and the subcooling temperature after the heat supply should be sufficiently low to guarantee the entire phase change material to solidify again before back into the cooling channels. Ho et al. [51, 52] experimentally studied the cooling performance of a minichannel heat sink with MPCS as the coolant. With the Reynolds number ranging from 133 to 1515, the thermal performance can be enhanced by addition of MEPCM particles, the case with lower flow rate and latent-sensible heat ratio had a better improvement of thermal resistance compared with the pure water, but the enhancement effect may be reduced by increasing the latent-sensible heat ratio.

Wu et al. [53] studied the heat transfer characteristics of NPCS. They concluded that slurry with encapsulated NPCM encountered a lower pressure drop and nearly the same heat transfer performance compared to the base fluid PAO. Results indicated that the heat transfer coefficient of slurry with 30% bare indium nanoparticle can reach 47 kW/m^2 K at flow rate of 3.5 ml/s (velocity of 0.28 m/s). The magnitude of heat transfer coefficient represented 2 times improvement over that of single phase PAO, and was also higher than that of single phase water. A thermal cycling test involving 5000 cycles showed a consistent performance of both types of slurries, due to the naturally developing oxide shell outside the particles, the surfactant used during the synthesis of particles, and residual charges which generated strong repulsive electrical force. As shown in Fig. 6, both bare and encapsulated NPCS attained 97% of their initial heat transfer performance after 5000 cycles. Sinha-Ray et al. [54] explored the heat transfer potential of NPCM (wax or meso-erythritol) in two microchannel heat sinks and found that the presence of the surfactant in CNT suspensions resulted in a pseudo-slip at the channel wall

which enhanced the flow rate at a fixed pressure drop. When aqueous surfactant were employed (with no CNTs added), the enhanced convection alone was responsible for an about 2 K reduction in temperature compared with pure water flows. When CNTs with nano-encapsulated wax were added, an additional about 1.9 K reduction in temperature due to the PCM fusion was observed when using 3 wt% CNT suspensions. These suspensions (1.5 wt% CNT) revealed a temperature reduction due to the PCM fusion of up to 3.2 K, and a fusion temperature in the range 118-120 °C.

4.3 Analytical and numerical investigations

Table 5 shows the key findings from recent analytical and numerical researches related to N/MPCS in mini/microchannel heat sinks in chorological order. Table 6 lists two numerical models for N/MPCS flowing in mini/microchannels mentioned below, including the two-phase model (heterogeneous) and the one-phase model (homogeneous).

Hao and Tao [55] developed the two-phase model to simulate the laminar flow and heat transfer of MPCS in a microchannel. The base fluid and the particles were separately treated as a liquid phase and a particle phase. Both of them were considered to be continuous and fully interpenetrating, and were described in terms of separated conservation equations with appropriate interaction terms representing the coupling between the two phases. The results with constant heat flux boundary conditions show that, the heat transfer coefficient increased streamwise and reached a peak in the melting region, and the preliminary results qualitatively agreed well with experimental measurements. They concluded that the benefits of heat transfer enhancement and wall temperature reduction by employing the PCM particle were mainly in the melting region, and an optimal design would match the microchannel geometric parameters, PCM volume fraction, Reynolds number, and the desired heat flux. Xing et al. [56] applied this two-phase, non-thermal-equilibrium model for the parametric study of optimal conditions considering both heat transfer and pumping power. They concluded that the main contribution of PCM particles to heat transfer enhancement in a microchannel was to increase the effective thermal capacity and utilized the latent heat under the laminar flow condition. For a given Reynolds number, there existed an optimal heat flux for the suspension flow which can have a significantly better heat transfer performance index than the base fluid. Fig. 7 demonstrates the local

heat transfer coefficient of such suspension flow at different Reynolds numbers for a given wall heat flux. Pattern difference of local heat transfer coefficient along the channel from pure liquid fluid was that a peak occurred, and the peak went toward the exit and became higher with the increase of Reynolds number.

Sabbah et al. [85] developed the one-phase, laminar flow model to investigate the thermal and hydraulic performance of MPCS in microchannel heat sinks. They found that a significant increase in the heat transfer coefficient under certain heat flux was mainly dependant on the channel inlet and outlet temperatures and the selected PCM melting temperature. Lower and more uniform temperatures across heat sink can be achieved at less pumping power for MPCS than the base fluid. To achieve high enhancement index for a certain heat flux, the cooling system should be designed that the phase change particles started melting right at the channel inlet and completely melted right at the channel exit. Kuravi et al. [58] used the one-phase model to analyse the heat transfer performance of N/MPCS in manifold microchannel heat sinks. Their model considered the microchannel fin or wall effect, axial conduction along the channel length, and the effect of developing flow. Influence of parameters such as particle concentration, inlet temperature, melting range of PCM, and heat flux was investigated. They observed that for a certain mass flow rate, an increased mass concentration of PCM resulted in an improvement of heat transfer performance, but larger pressure drop due to the increase of fluid effective viscosity. They also found that if the melting range was narrow, it was good to have the inlet temperature near the peak of the melting curve of the PCM. Hasan [57] used the one-phase model to study the fluid flow and heat transfer of N/MPCS in a microchannel heat exchanger. They found that such cooling fluid can modify the heat transfer performance by increasing the effectiveness but also lead to increased pressure drop. Dammel and Stephan [50] employed the one-phase model to investigate the heat transfer performance of laminar MPCS in rectangular copper minichannels. They suggested that the available latent heat storage potential should be in the same order of magnitude as the supplied heat, the residence time of the particles in the channels should be long enough in terms of the characteristic time for conduction perpendicular to the flow direction, and the inlet temperature of NPCS should be slightly below the theoretical melting temperature. They also studied the unfavourable characteristics of the MPCS such as higher viscosity, lower heat capacity, and lower thermal conductivity than basic fluid.

Fig. 8 demonstrates these influences on heat transfer performance through the computed temperature distribution at the channel outlet for three cases with different heat transfer rates and mass flow rates.

Alquaity et al. [59, 60] also investigated the heat transfer performance of laminar NPCS in rectangular microchannels with the one-phase model. They found that for a given particle concentration, an optimum heat flux to mass flow rate ratio existed that can lead to the maximum effectiveness ratio of 2.75, performance index of 1.37 and Merit number of 0.64 for their simulations. Fig. 9 shows the variation of effectiveness ratio, performance index and Merit number with ratio of heat flux to mass flow rate of such NPCS for different volume concentrations. Then, they introduced the discrete phase model (two-phase model) to the N/MPCS in a circle microchannel and compared with the one-phase model. As shown in Fig. 10, the discrete phase model indicated that presence of 10% volume concentration of PCM particles did not cause an increase of pressure drop along the channel length, while prediction from the one-phase model showed an increase of pressure drop due to the addition of nanoparticles where 10% volume concentration of particles caused 34.4% increase of pressure drop. The two models both predicted an improvement in the heat storage capacity due to the addition of PCM nanoparticles. They concluded that the discrete phase model was good at predicting the heat transfer due to the addition of nanoparticles, but it failed to accurately predict the pressure drop after the addition of nanoparticles into the base fluid. Seyf et al. [61] presented the thermal and hydrodynamic characteristics of NPCS in a microtube heat sink with tangential impingement using the one-phase model. The N/MPCS can result in a considerable heat transfer enhancement, but also induce drastic effects on pressure drop. An increase in nanoparticles mass concentration, inlet Reynolds number and melting range of PCM, resulted in a higher Nusselt number, better temperature uniformity, lower thermal resistance, and decreased entropy generation. Fig. 11 shows the effect of mass concentration of slurry on temperature distribution. It can be seen that the entrance length is longer for slurry flow that of pure PAO, due to the NPCM particles latent heat, which slows the growth of thermal boundary layer along the heat sink. Rajabifar et al. [62] employed the one-phase model to study the performance of NPCS in an enhanced microchannel heat sink with sectional oblique fins. They observed that in contrast with pure water, such slurry enhanced the cooling performance but increased the Euler number, which indicated that NPCS had the potential as effective substitutions for conventional coolants in order to

enhance the cooling performance of microchannel heat sinks, but there were usually a disadvantage that the increase of the needed pumping power of the system. Furthermore, if the tip clearance to channel width ratio was chosen properly for the heat sink, such slurry had the potential to enhance the cooling performance and reducing the Euler number simultaneously. Rajabifar [63] also investigated the performance of a double layer microchannel heat sink employing of NPCS and nanofluid coolants. Results showed that using the proposed configurations, the cooling performance of the systems were enhanced and the disadvantages associated with advanced coolant were substantially relieved.

5. Heat transfer and pressure drop correlations

The specific heat of N/MPCS changes drastically with temperature in the phase change process, and the subcooling enlarges the temperature range by decreasing the freezing point. Both of them lead to the difficulties to develop available heat transfer correlations for N/MPCS flowing in channels. Until now, only very few researchers have proposed empirical heat transfer correlations.

Based on their experimental data for different power inputs, flow conditions and slurry particle mass concentrations, Wang et al. [83] proposed an empirical heat transfer correlation which related to Shah and Londons' model for laminar single-phase flows in the developing region under a constant heat flux.

$$Nu_{\mathrm{Shan},x} = 5.364\left[1+\left(\frac{220}{\pi}\cdot\frac{x}{D_{\mathrm{h}}RePr}\right)^{-10/9}\right]^{3/10} - 1.0 \tag{28}$$

$$Nu_{\mathrm{MPCS}} = CNu_{\mathrm{Shan}} \tag{29}$$

where the values of C depends on the slurry particle fractions and C = 1.336, 1.341 and 1.418 respectively for c_{m} = 5%, 10% and 15.8%. Fig. 12 shows the comparison of their experimental data with those predicted by Eq. (29). It can be seen that all experimental data can be predicted within ±15%.

After carefully examined the dimensionless heat transfer correlations for water, Wang et al. [86] proposed correlations for MPCS in channels by the least square method with the regression analysis of their experiment data, with the following dimensionless numbers: *Re*, *Pr*, *Ste* and phase change region length $(L_1 + L_2) / D$.

For laminar MPCS flow with $60 < Re < 2200$, $12 < Pr < 73$, and $5\% < c_m < 27.6\%$

$$Nu = 0.8148 Re^{0.4593} Pr^{0.4836} Ste^{-0.1277} \left[(L_1 + L_2) / D_h \right]^{0.3059} \tag{30}$$

For turbulent MPCS flow with $2100 < Re < 3500$, $13 < Pr < 15$, and $5\% < c_m < 10\%$

$$Nu = 4.8527 \times 10^{-4} Re^{0.7733} Pr^{2.7941} Ste^{0.3159} \left[(L_1 + L_2) / D_h \right]^{-0.333} (\mu_b / \mu_w)^{-2.4349} \tag{31}$$

where the dimensionless group (μ_b/μ_w) is a correction factor to account for the effect of wall temperature on the heat transfer coefficient, and μ_b is the average dynamic viscosity of the slurry in the phase change region and μ_w is the average dynamic viscosity of water calculated based on the inner tube wall temperature. Comparison between their experimental data and the predictions with Eqs. (30) and (31), respectively for laminar and turbulent flow, showed these two correlations can predict their average heat transfer data with standard deviation within ±10%.

Based on their experimental work, Ho et al. [52] proposed a general heat transfer correlation for MPCS flowing in channels with the following parameters: Peclet number $Pe = Re\ Pr$, D_h, L, c_m, Ste and modified inlet subcooling parameter $Sb = (T_m - T_{in}) / \Delta T_{ref}$.

$$Nu = a\left(\frac{Pe}{L / D_h}\right)^b \left(1 + \frac{c_m}{Ste(1+Sb)}\right)^c \tag{32}$$

where the constants a, b, and c are listed in Table.7. Comparison between their experimental data and the predictions with Eq. (32) shows the maximum error 2.68%.

For pressure drop correlations, if the suspended particle size is very small and their volume concentrations are relatively low (less than 20-25%), the Newtonian flow assumption is valid for MPCS, which has been carefully discussed by Charunyakorn et al. [87], Roy and Avanic [84] and Wang et al. [83, 86]. The classical friction factors f were recommended for pressure drop calculation. For laminar MPCS flow, Wang et al. [86] suggested the classical model $f = 16 / Re$ based on Hagen-Poiseuille flow, and for turbulent MPCS flow, Wang et al. [86] recommended the modified Blasius equation $f = 0.12143 Re^{-0.25}$ and Roy and Avanic [84] recommended the classical Prandtl-Karman-Nikuradse correlation $f = \left[0.8686 \ln\left(\frac{Re}{1.964 \ln Re - 3.8215}\right) \right]^{-2}$, for pressure drop calculation during MPCS flowing in channels.

6. Conclusions

This paper presented a comprehensive review on the use of N/MPCS in mini/microchannel heat sinks. The research on mini/microchannel heat sinks has gained significant attention due to their higher heat transfer performance and the characteristics of compactness, small size and lesser weight. Due to requirement to remove more and more heat, recent technique of using N/MPCS as the heat transfer fluid in mini/microchannels is expected to further enhance the performance of such heat sink. The review is mainly focused on the material and thermophysical properties of N/MPCS used in mini/microchannels and their local, average and overall heat transfer and hydrodynamic performance with different composition and fraction of such slurry, different geometry of heat sink, and various operation conditions. N/MPCS in mini/microchannels can provide higher effective specific heat and heat transfer coefficient than base fluid owing to the latent heat, but the heat transfer performance of N/MPCS depends on various parameters such as base fluid thermal conductivity, channel dimensions, amount of specific heat used and the particle mass concentration, and the enhancement are partly offset by high pumping power of N/MPCS due to the increase in pressure drop and viscosity. Further, subcooling, durability and agglomeration of N/MPCS challenge their application in mini/microchannel heat sinks. And only very few researchers have proposed empirical heat transfer correlations useful for the design of compact heat exchangers with N/MPCS as working fluid.

7. Recommendations for future works

According to the investigations published in N/MPCS flowing in mini/microchannel heat sinks, several suggestions and recommendations are listed for future works: (i) Combine passive or active techniques in mini/microchannel heat sinks for further heat transfer augmentation, such as enhancing the heat transfer process by introduction of turbulence promoters to strengthen the mixing in the suspension flow or addition of nanoparticles with higher thermal conductivity to improve the thermal conductivity of the suspension. (ii) Optimize the operation parameters for given heat sink and N/MPCS, the available latent heat storage potential should be near the supplied heat, the residence time of the particles in the channels should be long enough for heat conduction and phase change, and the inlet

temperature of slurry should be slightly below the theoretical melting temperature. (iii) Concrete model of numerical simulation for a deeper understanding of the flow and heat transfer interactions is necessary that precisely take account for the force and effect of particle to base fluid, including gravity, friction between phases, Brownian diffusion, sedimentation, and dispersion. (iv) Present available studies do not cover as wide range of operation conditions required for universal heat transfer and pressure drop correlation development and compact heat exchanger design, thus more effort should be made to conduct experiment and simulation over a wider range of test parameters.

Acknowledgements

The work was supported by the Engineering and Physical Sciences Research Council (EPSRC) of the UK through research grants (EP/L001233/1 and RRR1025R33470) and the Youth Innovation Promotion Association of CAS (2016131).

1 **References**

2

[1] S.G. Kandlikar, W.J. Grande, Evolution of microchannel flow passages – thermohydraulic performance and fabrication technology. Heat Transfer Engineering, 24 (2003) 3-17.

[2] S. G. Kandlikar, S. Garimella, D. Li, S. Colin, M.R. King, Heat Transfer and Fluid Flow in Minichannels and Microchannels, Elsevier, 2005.

[3] L. Chai, G.D. Xia, L. Wang, Heat transfer enhancement in microchannel heat sinks with periodic expansion-constriction cross-sections, International Journal of Heat and Mass Transfer 62 (2013) 741-751.

[4] L. Chai, G.D. Xia, H.S. Wang, Numerical study of laminar flow and heat transfer in microchannel heat sink with offset ribs on sidewalls, Applied Thermal Engineering 92 (2016) 32-41.

[5] L. Chai, G.D. Xia, H.S. Wang, Laminar flow and heat transfer characteristics of interrupted microchannel heat sink with ribs in the transverse microchambers. International Journal of Thermal Sciences 110 (2016) 1-11.

[6] A.A. Hussien, M.Z. Abdullah, M.A. AI-Nimr, Single-phase heat transfer enhancement in micro/minichannels using nanofluids: Theory and applications, Applied Energy 164 (2016) 733-755.

[7] P. Li, S. Kuravi, Comparative study of thermal performance of liquid metal and water flow through a channel, In Proceedings of the International Conference on Research and Innovations in Mechanical Engineering (2014) 501-510, Springer, New Delhi.

[8] Y. Wang, Z. Chen, X. Ling, An experimental study of the latent functionally thermal fluid with micro-encapsulated phase change material particles flowing in microchannels, Applied Thermal Engineering 105 (2016) 209-216.

[9] G.D. Xia, L. Chai, M.Z. Zhou, Effects of structural parameters on fluid flow and heat transfer in a microchannel with aligned fan-shaped 21ehaviour21 cavities, International Journal of Thermal Sciences 50 (2011) 411-419.

[10] G.D. Xia, L. Chai, H.Y. Wang, Optimum thermal design of microchannel heat sink with triangular 22ehaviour22 cavities, Applied Thermal Engineering 31 (2011) 1208-1219.

[11] L. Chai, G.D. Xia, M.Z. Zhou, Optimum thermal design of interrupted microchannel heat sink with rectangular ribs in the transverse microchambers, Applied Thermal Engineering 51 (2013) 880-989.

[12] L. Chai, G.D. Xia, H.S. Wang, Parametric study on thermal and hydraulic characteristics of laminar flow in microchannel heat sink with fan-shaped ribs on sidewalls–Part 1: Heat transfer, International Journal of Heat and Mass Transfer 97 (2016) 1069-1080.

[13] J.K. Choi, J.G. Lee, J.H. Kim, H.S. Yang, Preparation of microcapsules containing phase change materials as heat transfer media by in-situ polymerization, Journal of Industrial and Engineering Chemistry 7 (2001) 358-362.

[14] Z. Jin, Y. Wang, J. Liu, Z. Yang, Synthesis and properties of paraffin capsules as phase change materials, Polymer 49 (2008) 2903-2910.

[15] L. Chen, T. Wang, Y. Zhao, X.R. Zhang, Characterization of thermal and hydrodynamic properties for microencapsulated phase change slurry (MPCS), Energy Conversion and Management 79 (2014) 317-333.

[16] G.L. Morini, Single-phase convective heat transfer in microchannels: a review of experimental results, International Journal of Thermal Sciences 43 (2004) 631-651.

[17] M.E. Steinke, S.G. Kandlikar, Review of single-phase heat transfer enhancement techniques for application in microchannels, minichannels and microdevices, International Journal of Heat and Technology 22 (2004) 3-11.

[18] P. Rosa, T.G. Karayiannis, M.W. Collins, Single-phase heat transfer in microchannels: the importance of scaling effects, Applied Thermal Engineering 29 (2009) 3447-3468.

[19] T. Dixit, I. Ghosh, Review of micro-and mini-channel heat sinks and heat exchangers for single phase fluids, Renewable and Sustainable Energy Reviews 41 (2015) 1298-1311.

[20] S. Kakaç, A. Pramuanjaroenkij, Single-phase and two-phase treatments of convective heat transfer enhancement with nanofluids–A state-of-the-art review, International Journal of Thermal Sciences 100 (2016) 75-97.

[21] M. Delgado, A. Lázaro, J. Mazo, B. Zalba, Review on phase change material emulsions and microencapsulated phase change material slurries: materials, heat transfer studies and applications, Renewable and Sustainable Energy Reviews 16 (2012) 253-273.

[22] P. Zhang, Z.W. Ma, R.Z. Wang, An overview of phase change material slurries: MPCS and CHS. Renewable and Sustainable Energy Reviews 14 (2010) 598-614.

[23] F. Gibbs, S. Kermasha, I. Alli, C.N. Mulligan, Encapsulation in the food industry: a review, International Journal of Food Sciences and Nutrition 50 (1999) 213-224.

[24] C.Y. Zhao, G.H. Zhang, Review on microencapsulated phase change materials (MEPCMs): fabrication, characterization and applications, Renewable and Sustainable Energy Reviews 15 (2011) 3813-3832.

[25] C. Liu, Z. Rao, J. Zhao, Y. Huo, Y. Li, Review on nanoencapsulated phase change materials: Preparation, characterization and heat transfer enhancement, Nano Energy 13 (2015) 814-826.

[26] A. Jamekhorshid, S.M. Sadrameli, M. Farid, A review of microencapsulation methods of phase change materials (PCMs) as a thermal energy storage (TES) medium, Renewable and Sustainable Energy Reviews 31 (2014) 531-542.

[27] Z. Qiu, X. Ma, P. Li, Micro-encapsulated phase change material (MPCM) slurries: Characterization and building applications, Renewable and Sustainable Energy Reviews 77 (2017) 246-262.

[28] N.H.S. Tay, M. Liu, M. Belusko, Review on transportable phase change material in thermal energy storage systems, Renewable and Sustainable Energy Reviews 75 (2017) 264-277.

[29] M.M.A. Khan, R. Saidur, F.A. Al-Sulaiman, A review for phase change materials (PCMs) in solar absorption refrigeration systems, Renewable and Sustainable Energy Reviews 76 (2017) 105-137.

[30] D.B. Tuckerman, R.F.W Pease, High-performance heat sinking for VLSI, IEEE Electron device letters 2 (1981) 126-129.

[31] M.J. Madou, Fundamentals of microfabrication: the science of miniaturization, CRC press, 2002.

[32] S. Ashman, S.G. Kandlikar, A review of manufacturing processes for microchannel heat exchanger fabrication, Proc. Fourth International Conference on Nanochannels, Microchannels and Minichannels (2006), Limerick, Ireland.

[33] N.H. Naqiuddin, L.H. Saw, M.C. Yew, Overview of micro-channel design for high heat flux application, Renewable and Sustainable Energy Reviews 82 (2018) 901-914.

[34] N.A.C. Sidik, M.N.A.W. Muhamad, W.M.A.A. Japar, An overview of passive techniques for heat transfer augmentation in microchannel heat sink, International Communications in Heat and Mass Transfer 88 (2017) 74-83.

[35] A. Dewan, P. Srivastava, A review of heat transfer enhancement through flow disruption in a microchannel, Journal of Thermal Science 24 (2015) 203-214.

[36] A.A. Rostami, A.S. Mujumdar, N. Saniei, Flow and heat transfer for gas flowing in microchannels: a review. Heat and Mass Transfer 38 (2002) 359-367.

[37] A. Agrawal, A comprehensive review on gas flow in microchannels. International Journal of Micro-Nano Scale Transport 2 (2012) 1-40.

[38] A.M. Adham, N. Mohd-Ghazali, R. Ahmad, Thermal and hydrodynamic analysis of microchannel heat sinks: A review, Renewable and Sustainable Energy Reviews 21 (2013) 614-622.

[39] J.R. Thome, Boiling in microchannels: a review of experiment and theory, International Journal of Heat and Fluid Flow 25 (2004) 128-139.

[40] L. Cheng, D. Mewes, Review of two-phase flow and flow boiling of mixtures in small and mini channels, International Journal of Multiphase Flow 32 (2006) 183-207.

[41] L. Cheng, G. Xia G, Fundamental issues, mechanisms and models of flow boiling heat transfer in microscale channels, International Journal of Heat and Mass Transfer 108 (2017) 97-127.

[42] T.G. Karayiannis, M.M. Mahmoud, Flow boiling in microchannels: Fundamentals and applications, Applied Thermal Engineering 115 (2017) 1372-1397.

[43] S.M. Kim, I. Mudawar, Review of databases and predictive methods for pressure drop in adiabatic, condensing and boiling mini/micro-channel flows, International Journal of Heat and Mass Transfer 77 (2014) 74-97.

[44] S.M. Kim, I. Mudawar, Review of databases and predictive methods for heat transfer in condensing and boiling mini/micro-channel flows, International Journal of Heat and Mass Transfer 77 (2014) 627-652.

[45] M.G. Khan, A. Fartaj, A review on microchannel heat exchangers and potential applications, International journal of energy research 35 (2011) 553-582.

[46] I. Mudawar, Two-phase microchannel heat sinks: theory, applications, and limitations, Journal of electronic packaging 133 (2011) 041002.

[47] Y. Rao, F. Dammel, P. Stephan, G. Lin, G. Flow frictional characteristics of microencapsulated phase change material suspensions flowing through rectangular minichannels, Science in China Series E: Technological Sciences 49 (2006) 445-456.

[48] Y. Rao, F. Dammel, P. Stephan, G. Lin, Convective heat transfer characteristics of microencapsulated phase change material suspensions in minichannels, Heat and Mass Transfer 44 (2007) 175-186.

[49] S. Kuravi, J. Du, L.C. Chow, Encapsulated phase change material slurry flow in manifold microchannels, Journal of Thermophysics and Heat Transfer 24 (2010) 364-373.

[50] F. Dammel, P. Stephan, Heat transfer to suspensions of microencapsulated phase change material flowing through minichannels, ASME Journal of Heat Transfer 134 (2012) 020907.

[51] C.J. Ho, W.C. Chen, W.M. Yan, Experimental study on cooling performance of minichannel heat sink using water-based MEPCM particles, International Communications in Heat and Mass Transfer 48 (2013) 67-72.

[52] C.J. Ho, W.C. Chen, W.M. Yan, Correlations of heat transfer effectiveness in a minichannel heat sink with water-based suspensions of Al_2O_3 nanoparticles and/or MEPCM particles, International Journal of Heat and Mass Transfer 69 (2014) 293-299.

[53] W. Wu, H. Bostanci, L.C. Chow, Y. Hong, C.M. Wang, M. Su, J.P. Kizito, Heat transfer enhancement of PAO in microchannel heat exchanger using nano-encapsulated phase change indium particles, International Journal of Heat and Mass Transfer 58 (2013) 348-355.

[54] S. Sinha-Ray, H. Sriram, A.L. Yarin, Flow of suspensions of carbon nanotubes carrying phase change materials through microchannels and heat transfer enhancement, Lab on a Chip 14 (2014) 494-508.

[55] Y.L. Hao, Y.X. Tao, A numerical model for phase-change suspension flow in microchannels, Numerical Heat Transfer, Part A: Applications 46 (2004) 55-77.

[56] K.Q. Xing, Y.X. Tao, Y.L. Hao, Performance evaluation of liquid flow with PCM particles in microchannels, ASME Journal of Heat Transfer 127 (2005) 931-940.

[57] M.I. Hasan, Numerical investigation of counter flow microchannel heat exchanger with MEPCM suspension, Applied Thermal Engineering 31 (2011) 1068-1075.

[58] S. Kuravi, K.M. Kota, J. Du, L.C. Chow, Numerical investigation of flow and heat transfer performance of nano-encapsulated phase change material slurry in microchannels, ASME Journal of Heat Transfer 131 (2009) 062901.

[59] A.B.S. Alquaity, S.A. Al-Dini, E.N. Wang, B.S. Yilbas, Numerical investigation of liquid flow with phase change nanoparticles in microchannels, International Journal of Heat and Fluid Flow 38 (2012) 159-167.

[60] A.B.S. Alquaity, S.A. Al-Dini, B.S. Yilbas, Investigation into thermal performance of nanosized phase change material (PCM) in microchannel flow, International Journal of Numerical Methods for Heat & Fluid Flow 23 (2013) 233-247.

[61] H.R. Seyf, Z. Zhou, H.B. Ma, Y. Zhang, Three dimensional numerical study of heat-transfer enhancement by nano-encapsulated phase change material slurry in microtube heat sinks with tangential impingement, International Journal of Heat and Mass Transfer 56 (2013) 561-573.

[62] B. Rajabifar, S.K. Mohammadian, S.K. Khanna, Y. Zhang, Effects of pin tip-clearance on the performance of an enhanced microchannel heat sink with oblique fins and phase change material slurry, International Journal of Heat and Mass Transfer 83 (2015) 136-145.

[63] B. Rajabifar, Enhancement of the performance of a double layered microchannel heatsink using PCM slurry and nanofluid coolants, International Journal of Heat and Mass Transfer 88 (2015) 627-635.

[64] Y. Yamagishi, T. Sugeno, T. Ishige, H. Takeuchi, A.T. Pyatenko, An evaluation of microencapsulated PCM for use in cold energy transportation medium, Energy conversion engineering conference, IECEC 96, Proceedings of the 31st intersociety, 1996, 2077-2083.

[65] R. Yang, H. Xu, Y. Zhang, Preparation, physical property and thermal physical property of phase change microcapsule slurry and phase change emulsion, Solar Energy Materials & Solar Cells 80 (2003) 405-416.

[66] W. Li, X.X. Zhang, X.C. Wang, J.J. Niu, Preparation and characterization of microencapsulated phase change material with low remnant formaldehyde content, Materials Chemistry and Physics 106 (2007) 437-442.

[67] C. Alkan, A. Sarı, A. Karaipekli, O. Uzun, Preparation, characterization, and thermal properties of microencapsulated phase change material for thermal energy storage, Solar Energy Materials & Solar Cells 93 (2009) 143-147.

[68] A. Sarı, C. Alkan, A. Karaipekli, Preparation, characterization and thermal properties of PMMA/n-heptadecane microcapsules as novel solid–liquid microPCM for thermal energy storage, Applied Energy 87 (2010) 1529-1534.

[69] B.J. Chen, X. Wang, R.L. Zeng, Y.P. Zhang, X.C. Wang, J.L. Niu, An experimental study of convective heat transfer with microencapsulated phase change material suspension: laminar flow in a circular tube under constant heat flux, Experimental Thermal and Fluid Science 32 (2008) 1638-1646.

[70] B.C. Pak, Y.I. Cho, Hydrodynamic and heat transfer study of dispersed fluids with submicron metallic oxide particles. Experimental Heat Transfer an International Journal 11 (1998) 151-170.

[71] J.C. Maxwell, A treatise on electricity and magnetism, Cambridge, 1904.

[72] R.L. Hamilton, O.K. Crosser, Thermal conductivity of heterogeneous two-component systems, Industrial & Engineering Chemistry Fundamentals 1 (1962) 187-191.

[73] C.J. Ho, J.B. Huang, P.S. Tsai, Y.M. Yang, Water-based suspensions of Al_2O_3 nanoparticles and MEPCM particles on convection effectiveness in a circular tube, International Journal of Thermal Sciences 50 (2011) 736-748.

[74] L. Wang, G. Lin, Experimental study on the convective heat transfer 28 ehaviour of microencapsulated phase change material suspensions in rectangular tube of small aspect ratio, Heat and Mass Transfer 48 (2012) 83-91.

[75] G.H. Zhang, C.Y. Zhao, Thermal and rheological properties of microencapsulated phase change materials, Renewable Energy 36 (2011) 2959-2966.

[76] M. Goel, S.K. Roy, S. Sengupta, Laminar forced convection heat transfer in microcapsulated phase change material suspensions, International Journal of Heat and Mass Transfer 37 (1994) 593-604.

[77] S. Mossaz, J.A. Gruss, S. Ferrouillat, J. Skrzypski, D. Getto, O. Poncelet, P. Berne, Experimental study on the influence of nanoparticle PCM slurry for high temperature on convective heat transfer and energetic performance in a circular tube under imposed heat flux, Applied Thermal Engineering 81 (2015) 388-398.

[78] A. Einstein, Investigations on the theory of the Brownian movement, Courier Corporation, 1956.

[79] G. Batchelor G, The effect of Brownian motion on the bulk stress in a suspension of spherical particles, Journal of Fluid Mechanics 83 (1977) 97-117.

[80] V. Vand, Theory of viscosity of concentrated suspensions, Nature 155 (1945) 364-365.

[81] J.C. Mulligan, D.P. Colvin, Y.G. Bryan, Microencapsulated phase change material suspensions for heat transfer in spacecraft thermal systems, Journal of Spacecraft and Rockets 33 (1996) 278-284.

[82] Y. Yamagishi, H. Takeuchi, A.T. Pyatenko, Characteristics of microencapsulated PCM slurry as a heat-transfer fluid, AIChE Journal 45 (1999) 696-707.

[83] X. Wang, J. Niu, Y. Li, X. Wang, B. Chen, R. Zeng, Y. Zhang, Flow and heat transfer behaviors of phase change material slurries in a horizontal circular tube, International Journal of Heat and Mass Transfer 50 (2007) 2480-2491.

[84] S.K. Roy, B.L. Avanic, Turbulent heat transfer with phase change material suspensions, International Journal of Heat and Mass Transfer 44 (2001) 2277-2285.

[85] R. Sabbah, M.M. Farid, S. Al-Hallaj, Micro-channel heat sink with slurry of water with micro-encapsulated phase change material: 3D-numerical study, Applied Thermal Engineering 29 (2008) 445-454.

[86] X. Wang, J. Niu, Y. Li Y. Heat transfer of microencapsulated PCM slurry flow in a circular tube. AIChE Journal 54 (2008) 1110-1120.

[87] Charunyakorn P, Sengupta S, Roy S K. Forced convection heat transfer in microencapsulated phase change material slurries: flow in circular ducts. International Journal of Heat and Mass Transfer 34 (1991) 819-833.

1

2

Nomenclature

a	parameter in Eq. (32)
A	parameter in Eq. (18); area, m^2
b	parameter in Eq. (32)
B	parameter in Eq. (9)
c	concentration, parameter in Eq. (32)
c_p	specific heat, $J \cdot kg^{-1} K^{-1}$
d	diameter, m
D_h	hydraulic diameter, m
e	shear rate magnitude, s^{-1}
Eu	Euler number
$\vec{F}$	force, N
f	friction factor
h	heat transfer coefficient, $W \cdot m^{-2} \cdot K^{-1}$
h_{sf}	latent heat of PCM particles, $J \cdot kg^{-1}$
k	thermal conductivity, $W \cdot m^{-1} \cdot K^{-1}$
L	length, m
m	parameter in Eq. (9), mass flow rate, $kg \cdot s^{-1}$
Me	Merit number
n	shape factor; number of channels
Nu	Nusselt number
p	pressure, Pa
P	pumping power, W
Pe	Peclet number
Pr	Prandtl number
q	heat flux, $W \cdot m^{-2}$
Q	heat transfer rate, W

Re	Reynolds number
S	heat, W
Sb	modified inlet subcooling parameter
Ste	Stephen number
S'''_{gen}	volume entropy generation, $W \cdot m^{-3} \cdot K^{-1}$
T	temperature, K
T_1	lower melting temperature, K
T_2	higher melting temperature, K
T_{mr}	melting range ($T_{mr} = T_2 - T_1$), K
v	velocity, $m \cdot s^{-1}$
V	volume, m^3
W	width, m
y	core-shell weight ratio
x	length along the channel, m
x^+	non-dimensional length $x^+ = 2x/(D_h Re\ Pr)$
x,y,z	coordinates, m
Δp	pressure drop, Pa
ΔT	temperature difference, K
Greek letters	
α	thermal diffusivity, $m^2 \cdot s^{-1}$
γ	shear rate, s^{-1}
η	performance index
ρ	density, $kg \cdot m^{-3}$
μ	dynamic viscosity, Pa·s
v	kinematic viscosity, $m^2 \cdot s^{-1}$
Subscripts	
b	slurry

c	core
f	base fluid
m	mass, mean
p	particle
ref	reference
s	shell
v	volume
w	wall
Abbreviations	
CNTs	carbon nanotubes
MPCM	microencapsulated phase change material
NaDDBS	sodium dodecyl benzene sulfonate
NPCM	nanoencapsulated phase change material
NPCS	nanoencapsulated phase change slurry
N/MPCS	nano/microencapsulated phase change slurry
PAO	poly-a-olefin
PCM	phase change material
PCS	phase change slurry
PMMA	polymethyl methacrylate

1

2

Table captions

Figure captions

Table 1 Representative properties of N/MPCS flowing in mini/microchannels from experimental researches.

References	Base fluid	Core material	Shell material	Size distribution	Phase change temperature	Phase change enthalpy, kJ/kg
Rao et al. [47, 48]	water	*n*-octadecane	PMMA	4.97 μm	28 °C	latent heat: 241 kJ/kg
Kuravi et al. [49]	water	*n*-octadecane	PMMA	1-5 μm	23-29 °C	latent heat: 120 kJ/kg
Dammel and Stephan [50]	water	*n*-eicosane	PMMA	1.5-12 μm	36.4 °C	latent heat: 247.3 kJ/kg
Ho et al. [51, 52]	water	*n*-eicosane		4-10 μm	melting temperature: 35.8-36.4 °C freezing temperature: 34.0-34.7 °C	
Wu et al. [53]	PAO	tetraethoxysilane	silicon	150-1000 nm	melting temperature: 155 °C freezing temperature: 135 °C	silica encapsulated indium nanoparticles: 19.6 kJ/kg pure indium nanoparticles: 38.5 kJ/kg
Sinha-Ray et al. [54]	alpha-olefin oil	wax or meso-erythritol	carbon nanotubes (CNTs)	nano	wax: 40-80 °C meso-erythritol: 118-120 °C	wax:~200 kJ/kg meso-erythritol:~300 kJ/kg

Table 2 Representative properties of N/MPCS flowing in mini/microchannels from analytical and numerical researches.

References	Base fluid	Core material	Shell material	Size distribution	Phase change temperature	Phase change enthalpy (latent heat)
Hao and Tao [55]	water	*n*-octadecane	melamine-formaldehyde resinous	0.244-10 μm		167 kJ/kg
Xing et al. [56]	water	*n*-octadecane	melamine-formaldehyde resinous	6.3 μm	301 K	223 kJ/kg
Kuravi et al. [49]	water and PAO	*n*-octadecane		4.97 μm	23-33 °C	244 kJ/kg
Hasan [57]	water	*n*-octadecane	PMMA		melting temperature: 300-305 K	245 kJ/kg
Dammel and Stephan [50]	water	*n*-eicosane	PMMA	1.5-12 μm	36.4 °C	247.3 kJ/kg
Kuravi et al. [58]	PAO	*n*-octadecane		nano	301.9 K	247 kJ/kg
Alquaity et al. [59, 60]	water	lauric acid		nano	melting temperature: 317.2 K	211 kJ/kg
Seyf et al. [61]	PAO	*n*-octadecane		nano	301.9 K	244 kJ/kg
Rajabifar. et al. [62]	water	*n*-octadecane		nano	296.15-306.15 K	244 kJ/kg
Rajabifar. et al. [63]	water	*n*-octadecane		100 nm	296.15-306.15 K	244 kJ/kg

Table 3 Non-dimensional numbers relevant to mini/microchannel heat sinks with N/MPCS flowing inside.

Non-dimensional number	Significance
Nusselt number $Nu = \frac{hD_{\mathrm{h}}}{k_{\mathrm{b}}}$	Thermal resistance ratio of conductive to convective heat transfer, a significant number to provide a measure of the convection heat transfer occurring at the surface.
Prandtl number $Pr = \frac{\upsilon}{\alpha}$	Ratio of the kinematic viscosity to the thermal diffusivity, a significant number of estimating the relative effectiveness of momentum and energy transport by diffusion in the velocity and thermal boundary layers.
Reynolds number $Re = \frac{\rho_{\mathrm{b}} v D_{\mathrm{h}}}{\mu_{\mathrm{b}}}$	Ratio of the inertia to viscous forces, a significant number to study pressure drop and pumping power.
Darcy friction factor $f = \frac{\Delta p D_{\mathrm{h}}}{2\rho_{\mathrm{b}} L v^2}$	Ratio of the local shear stress to the local flow kinetic energy density, a significant number to study pressure drop and pumping power.
Stephen number $Ste = \frac{c_{\mathrm{p,b}}(T_{\mathrm{b,o}} - T_{\mathrm{b,i}}) - h_{\mathrm{sf}}}{h_{\mathrm{sf}}} = \frac{q_{\mathrm{w}}}{m h_{\mathrm{sf}}} - 1$	Ratio of the sensible heat to the latent heat, a significant number of estimating the efficiency of N/MPCS.
Euler number $Eu = \frac{2\Delta p}{\rho_{\mathrm{b}} Re^2 n}$	Dimensionless parameter related to the ratio of pressure drop of the system and squared Reynolds number.
Performance index $\eta = \frac{(Q/P)_{\mathrm{b}}}{(Q/P)_{\mathrm{f}}}, P_{\mathrm{b}} = \Delta p_{\mathrm{b}} V_{\mathrm{b}} A_{\mathrm{flow}}, P_{\mathrm{f}} = \Delta p_{\mathrm{f}} V_{\mathrm{f}} A_{\mathrm{flow}}$	Energy ratio of improvement to evaluate the transported thermal energy compared with basic fluid at an equal pumping power.

Effectiveness ratio $\varepsilon = \frac{Q_b}{Q_f},\ Q_b = qLW,\ Q_f = \dot{m} c_{p,f} \Delta T_f$	Ratio of heat transfer rate of N/MPCS to that of base fluid for the same temperature rise from inlet to exit of the channel.
Merit number $Me = \frac{Q_{gain}}{Q_b + P},\ Q_{gain} = Q_b - Q_f,\ P = S''_{gen} V T_{ref},\ S''_{gen} = \frac{k_b}{T^2}\left[(\frac{\partial T}{\partial x})^2 + (\frac{\partial T}{\partial x})^2 \right] + \frac{\mu_b}{T} (\frac{\partial u}{\partial y})^2$	Ratio of the gain in heat transfer due to use of phase change particles to the sum of heat transferred in the channel and the irreversibility.

Table 4 Representative heat transfer and hydrodynamic studies of N/MPCS flowing in mini/microchannels from experimental researches.

References	Flow condition	Test section material	Test section dimension	N/MPCS	Fraction	Measured characteristics	Remarks
Rao et al. [47]	laminar $200<Re<2000$	copper	rectangular $W = 2$ mm $H = 4.2$ mm $L = 150$ mm $D_h = 2.71$ mm	*n*-octadecane/water	c_m, 0-20%	Average pressure drop	The suspensions with 0 and 5% concentration agree well with the existing theoretical data for laminar Newtonian flow. For the suspensions with mass concentrations higher than 10%, there is an obvious increase in friction factor and pressure drop in comparison with laminar Newtonian flow.
Rao et al. [48]	laminar	copper	rectangular $W = 2$ mm $H = 4.2$ mm $L = 150$ mm $D_h = 2.71$ mm	*n*-octadecane/water	c_m, 0-20%	Local and average heat transfer	The cooling performance of the suspension strongly depends on the mass flow rate and the MEPCM mass concentration. The suspensions with higher mass concentrations are more effective only at low mass flow rates. At higher mass flow rates they show a less effective cooling performance than water.
Kuravi et al. [49]	laminar	copper	rectangular $W = 101$ μm $H = 533$ μm $L = 1$ mm $D_h = 170$ μm	*n*-octadecane/water	c_m, 10%	Average pressure drop and heat transfer	For developing flows, the performance of slurry depends on various parameters such as base fluid thermal conductivity, channel dimensions, amount of specific heat used and the particle mass concentration.
Dammel and	laminar $19<Re<367$	copper	rectangular $W = 2$ mm $H = 4.2$ mm	*n*-eicosane/water	c_m, 10% and 20%	Average pressure drop, local and	The particles are not evenly distributed in the flowing suspension, but there is a particle-depleted layer close to the channel walls, which reduces the required

Stephan [50]			L = 390 mm D_h = 2.71 mm			average heat transfer	pumping power while conducts a sufficiently large amount of the supplied heat to the center region.
Ho et al. [51, 52]	laminar 133<Re<1515	copper	rectangular W = 1 mm H = 1.5 mm L = 150 mm D_h = 1.2 mm	water-based suspensions of Al_2O_3 nanoparticles and/or MEPCM particles	c_m, 0-10%	Average pressure drop and heat transfer	The heat transfer effectiveness of incorporating the nanofluid and MPCM suspension in minichannel heat sink depends on the flow rate, the particle fraction dispersed in water, and the latent–sensible heat ratio of the MPCM suspension.
Wu et al. [53]	laminar	copper	rectangular W = 25 and 100 μm H = 500 μm L = 1 mm	tetraethoxysilane/ poly-a-olefin	c_m, 9% and 30%	Average pressure drop and heat transfer	The magnitude of heat transfer coefficient represents 2 times improvement over that of single phase PAO, and is also higher than that of single phase water.
Sinha-Ray et al. [54]	laminar	stainless steel	circle D = 603 and 1803 μm	wax or mesoerythritol/ alpha-olefin oil	c_m, 0-3%	Average pressure drop and heat transfer	The presence of the surfactant NaDDBS in water leads to an apparent slip at the channel walls, which can enhance the convective heat removal from a hot copper block. The presence of wax inside CNTs can facilitate heat removal through the latent heat of wax fusion.

Table 5 Representative heat transfer and hydrodynamic studies of N/MPCS flowing in mini/microchannels from analytical and numerical researches.

References	Flow condition	Test section material	Test section dimension	N/MPCS	Fraction	Remarks
Hao and Tao [55]	laminar Re = 100, 167		circular D = 122 μm L = 12.2 mm	*n*-octadecane/water	c_v, 25%	The introduction of PCM particles strongly enhances the heat transfer in the melting region. An optimal design would match the microchannel geometric parameters, PCM fraction, and Reynolds number with the desired heat flux.
Xing et al. [56]	laminar Re = 90, 167, 300, 600	silver	circular D = 122 μm L = 12.2 mm	*n*-octadecane/water	c_v, 15% and 25%	PCM suspension has a significantly higher performance index than the base fluid flow. For a given Reynolds number, there exists an optimal heat flux under which the effectiveness factor is the greatest.
Sabbah et al. [85]	laminar Re = 80, 158, 236	copper aluminium	rectangular W = 100 μm H = 500 μm L = 10.0 mm D_h = 160 μm	*n*-octadecane/water	c_v, 5-25%	A significant increase in the heat transfer coefficient under certain conditions mainly dependant on the channel inlet and outlet temperatures and the selected PCM melting temperature.
Kuravi et al. [49]	laminar	copper	rectangular W = 101 and 25 μm H = 533 and 375 μm L = 1 mm D_h = 170 AND 47 μm	*n*-octadecane /water or PAO	c_m, 0-30%	For developing flows, the performance of slurry depends on various parameters such as base fluid thermal conductivity, channel dimensions, amount of specific heat used and the particle mass concentration.

Hasan [57]	laminar	aluminium	rectangular W = 100 μm H = 500 μm L = 10.0 mm D_h = 166.6 μm	*n*-octadecane/water	c_v, 2-20%	PCM suspensions modify the thermal performance of a microchannel heat sink by increasing its effectiveness but also increased pressure drop.
Dammel and Stephan [50]	laminar 19<Re<367	copper	rectangular W = 2 mm H = 4.2 mm L = 390 mm D_h = 2.71 mm	*n*-eicosane/water	c_m, 10% and 20%	The measured pressure drop is smaller than that estimated by the measured viscosities, and the difference increases with increasing particle mass fraction, showing that the particles are not evenly distributed in the flowing suspension.
Kuravi et al. [58]	laminar Re = 200	copper	rectangular W = 100 μm H = 500 μm L = 1 mm	*n*-eicosane/water or PAO	c_m, 0-30%	The narrow melting range is good to have the inlet temperature near the peak of the melting curve of the PCM. The difference in the performance of the slurry and PAO increases with an increase of heat flux.
Alquaity et al. [59]	laminar Re = 691 and 1418		rectangular W = 2 mm H = 50 μm L = 35 mm	lauric acid/ water	c_v, 0-10%	For a given particle concentration, an optimum heat flux to mass flow rate ratio exists that leads to the best heat transfer performance.
Alquaity et al. [60]	laminar Re = 200		circle D = 50 μm L = 35 mm	lauric acid/ water	c_v, 0-10%	The discrete phase model indicates that presence of 10% volume concentration of PCM particles does not cause an increase in the pressure drop along the channel, while the homogeneous model shows a 34.4% increase in pressure drop.
Seyf et al. [61]	laminar Re = 200, 400, 600	silicon	circular D = 300 μm L = 1 mm	*n*-octadecane/ polyalphaolefin	c_m, 10-30%	Adding NPCM to base fluid leads to considerable heat transfer enhancement, which increases with an increase of nanoparticles mass concentration, inlet Reynolds number and

						melting range. NPCM slurry induces drastic effects on the pressure drop that increases with mass concentration and Reynolds number.
Rajabifar et al. [62]	laminar $Re < 215$	Copper	microchannel with oblique fins D_h = 537 and 539 μm	*n*-Octadecane/ water	c_v, 0-30%	NPCM slurry enhances the cooling performance of the heat sink but increases the Euler number. Introduction of tip-clearance to the heat sink has the potential to enhance the cooling performance and reduce the Euler number simultaneously.
Rajabifar [63]	laminar	silicon	double layered microchannel W = 53-61 μm H = 243-284 μm L = 100 mm	*n*-Octadecane/ water	c_v, 0-30%	NPCM slurries may boost up the cooling performance of the system by slowing the thermal boundary layer development while nanofluids improve it through enhancing the average thermal conductivity of the coolant.

Table 6 The two-phase model and the one-phase model.

Two-phase model	One-phase model
The base fluid and the encapsulated particles are treated as a liquid phase and a particle phase, respectively. Continuity equation: $\nabla \cdot (c_v \rho_p \vec{u}) = 0$ (19) $\nabla \cdot \left[(1-c_v) \rho_f \vec{u} \right] = 0$ (20) Momentum equation: $\nabla \cdot \left(c_v \rho_p \vec{u}\vec{u} \right) = -c_v \nabla p + \nabla \cdot \left[c_v \mu_p (\nabla \vec{u} + \nabla \vec{u}^T) \right] + \vec{F}_{fp}$ (21) $\nabla \cdot \left[(1-c_v) \rho_f \vec{u}\vec{u} \right] = -(1-c_v) \nabla p + \nabla \cdot \left[(1-c_v) \mu_f (\nabla \vec{u} + \nabla \vec{u}^T) \right] + \vec{F}_{pf}$ (22) Energy equation: $\nabla \cdot \left(c_v \rho_p c_{p,p} \vec{u} T \right) = \nabla \cdot \left(c_v k_p \nabla T \right) + c_v \mu_p (\nabla \vec{u} + \nabla \vec{u}^T) \cdot \nabla \vec{u} + S_{fp}$ (23) $\nabla \cdot \left[(1-c_v) \rho_f c_{p,f} \vec{u} T \right] = \nabla \cdot \left[(1-c_v) k_f \nabla T \right] + (1-c_v) \mu_f (\nabla \vec{u} + \nabla \vec{u}^T) \cdot \nabla \vec{u} + S_{pf}$ (24) where $\vec{F}_{fp} = -\vec{F}_{pf}$ is the forces acting on the encapsulated particles from the base fluid, including the drag force and the virtual mass force; $S_{fp} = -S_{pf}$ is the heat transfer from the base fluid to the encapsulated particles.	The base fluid and the encapsulated particles are assumed to have the same temperature and velocity. Continuity equation: $\nabla \cdot (\rho_b \vec{u}) = 0$ (25) Momentum equation: $\nabla \cdot \left(\rho_b \vec{u}\vec{u} \right) = -\nabla p + \nabla \cdot \left[\mu_b (\nabla \vec{u} + \nabla \vec{u}^T) \right]$ (26) Energy equation: $\nabla \cdot \left(\rho_b c_{p,b} \vec{u} T \right) = \nabla \cdot \left(k_b \nabla T \right) + \mu_b (\nabla \vec{u} + \nabla \vec{u}^T) \cdot \nabla \vec{u}$ (27)

Table 7 Constants in the correlation Eq. (32) proposed by Ho et al. [52].

	a	*b*	*c*
665<*Pe*<3250	8.193	-0.022	-0.112
3250<*Pe*<4550	1.383	0.409	0.012
4550<*Pe*<7550	4.667	0.155	0.034

Fig. 1 Microchannel heat sinks [2].

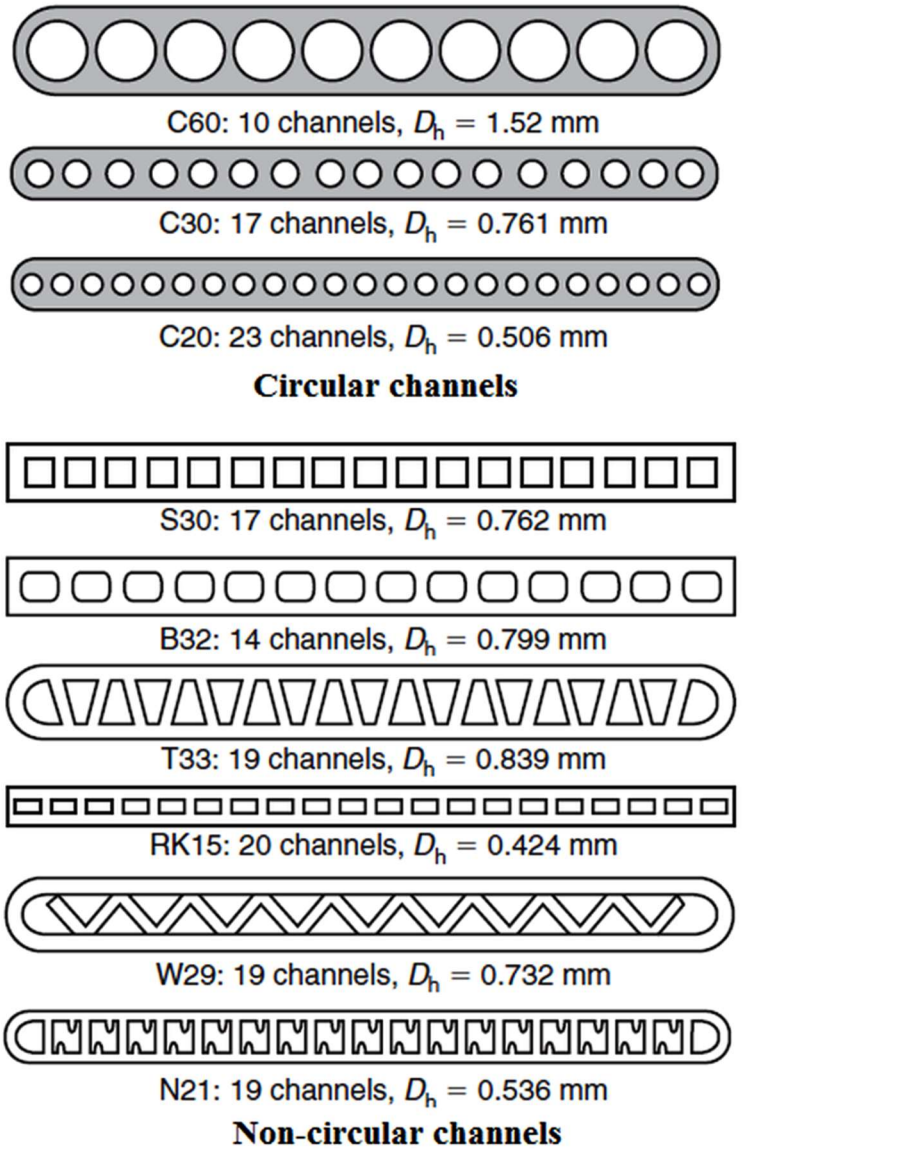

* Provided by Modine Manufacturing Company of Racine, Wisconsin

* C: circle, drawn; S: square, extruded; B: barrel, extruded; T: triangle, extruded; RK: rectangle, extruded; W: triangle, insert; N: N shape, extruded

Fig. 2 SEM images of two types of phase change particle. (a) microencapsulated phase change particles [48] and (b) nanoencapsulated phase change particles [53].

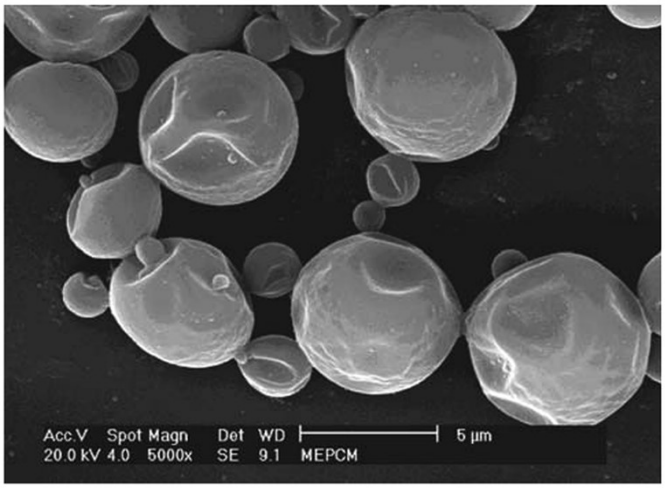

(a)

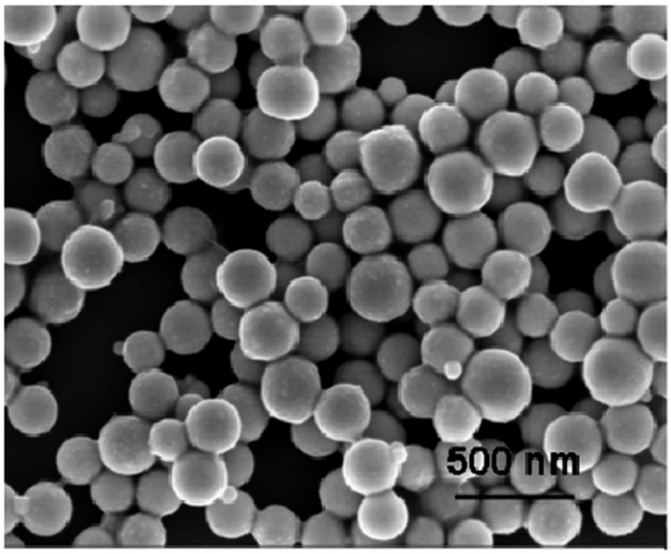

(b)

Fig. 3 Predicted specific heat profiles of $c_{p,p}$ and $c_{p,b}$ in the melting region. (a) $c_{p,p}$, (b) $c_{p,b}$ with Eqs. (12) and (14) and (c) $c_{p,b}$ with Eqs. (12) and (15).

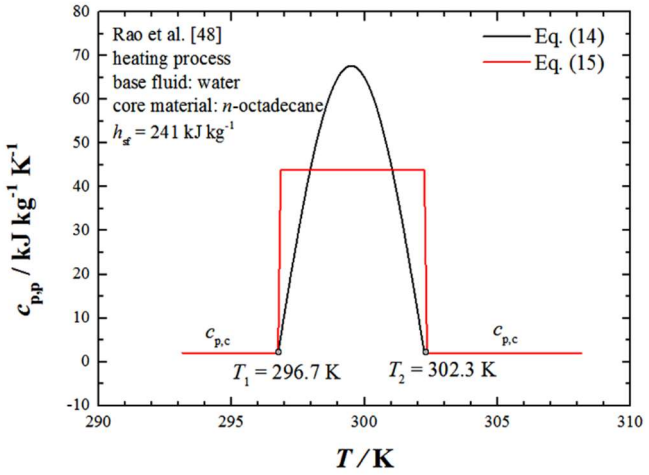

(a)

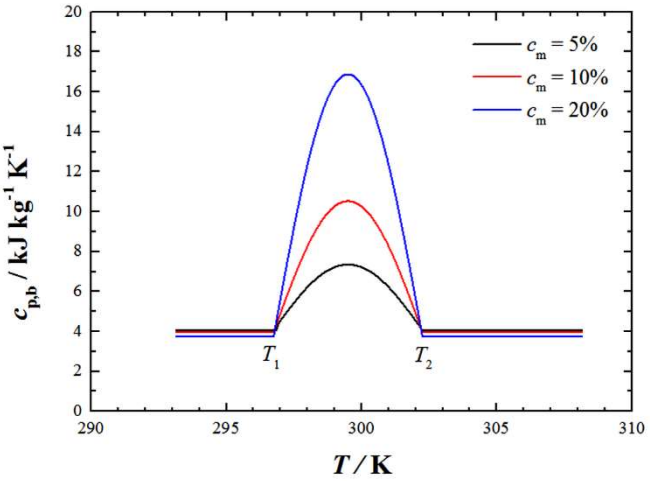

(b)

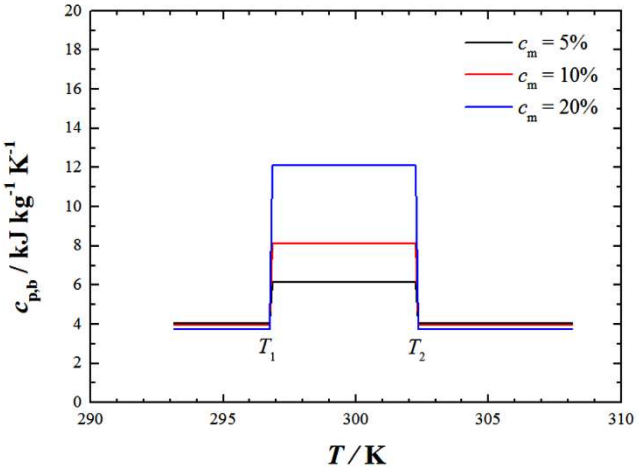

(c)

Fig. 4 Profiles of predicted effective viscosity of N/MPCS.

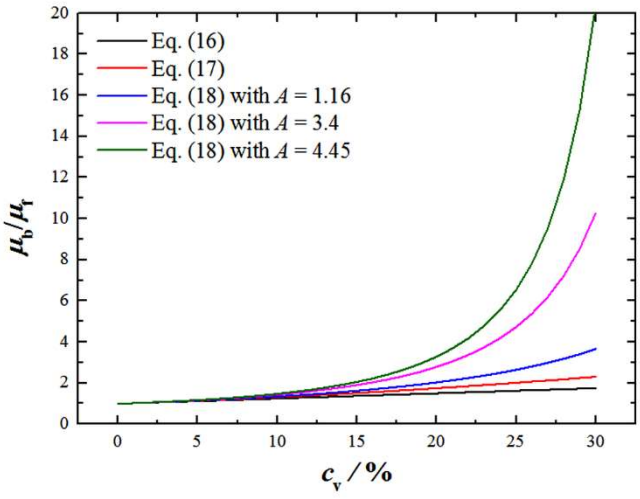

Fig. 5 Nu_b/Nu_f and $\Delta p_b/\Delta p_f$ with different mass concentrations [47, 48]. (a) Nu_b/Nu_f with c_m and (b) $\Delta p_b/\Delta p_f$ with c_m.

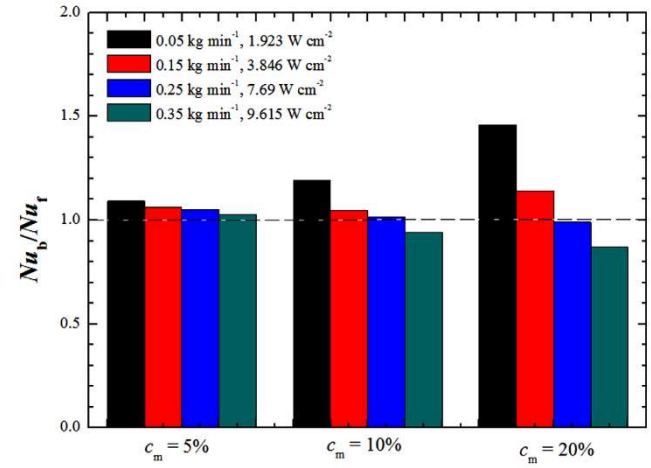

(a)

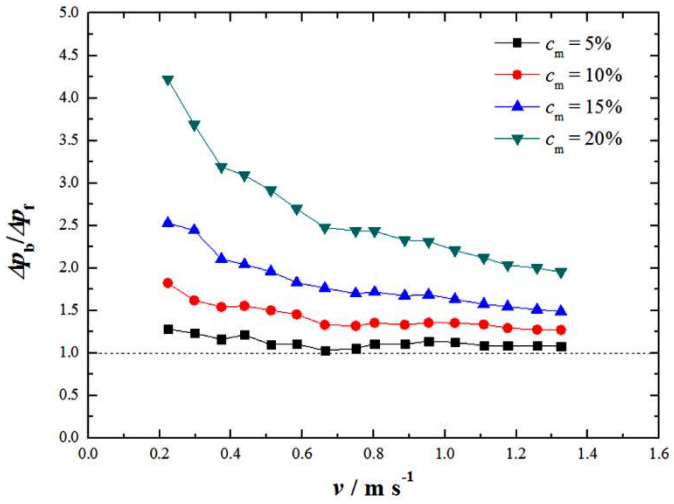

(b)

Fig. 6 Change of heat transfer performance of N/MPCS during 5000 thermal cycling [53].

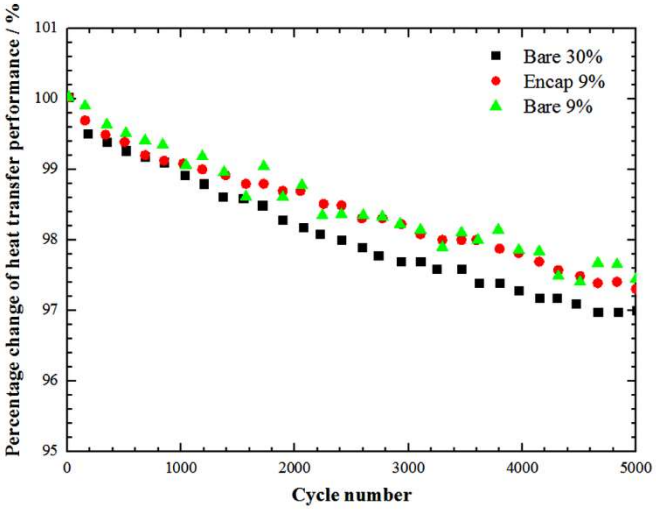

Fig. 7 Local heat transfer coefficient of N/MPCS along the channel [56].

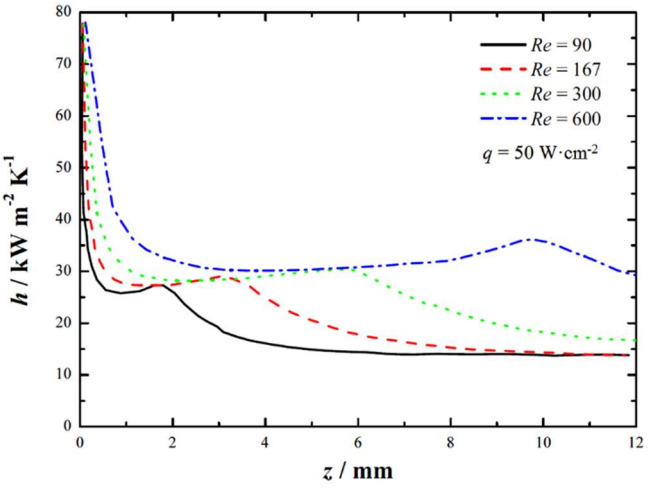

Fig. 8 Temperature distribution at the channel outlet of N/MPCS with c_m =20% [50].

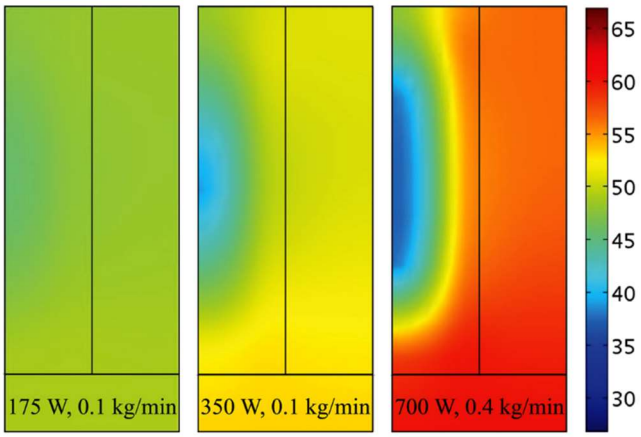

Fig. 9 Variation of effectiveness ratio, performance index and Merit number with ratio of heat flux to mass flow rate of N/MPCS [59].

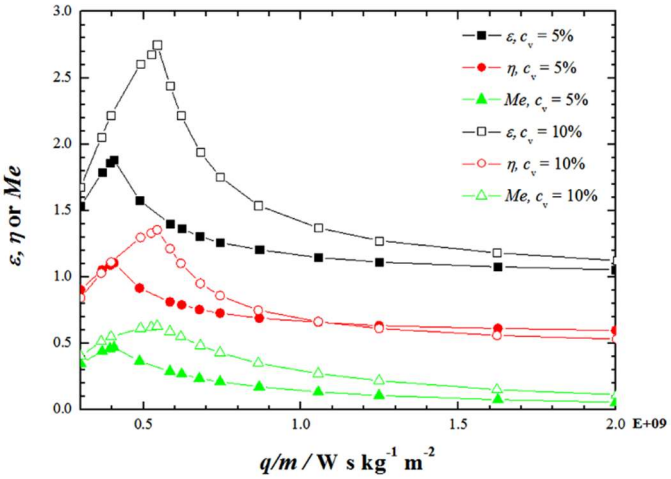

Fig. 10 Comparison of Nusselt number and pressure drop between two-phase model and one-phase model [60]. (a) Nusselt number and (b) pressure drop.

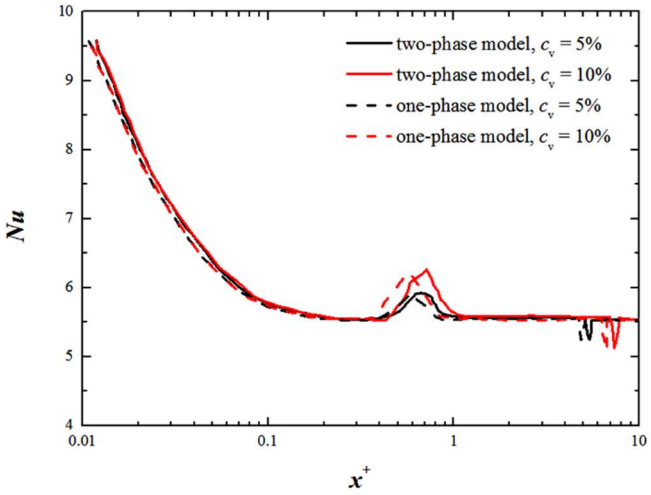

(a)

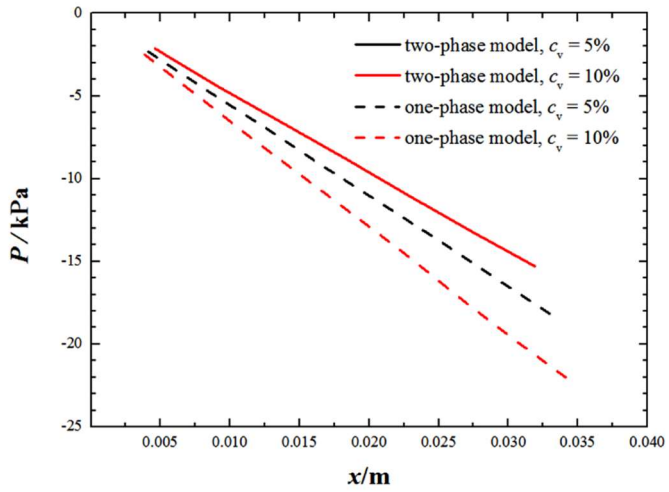

(b)

Fig. 11 Effect of mass concentration of slurry on temperature distribution [61].

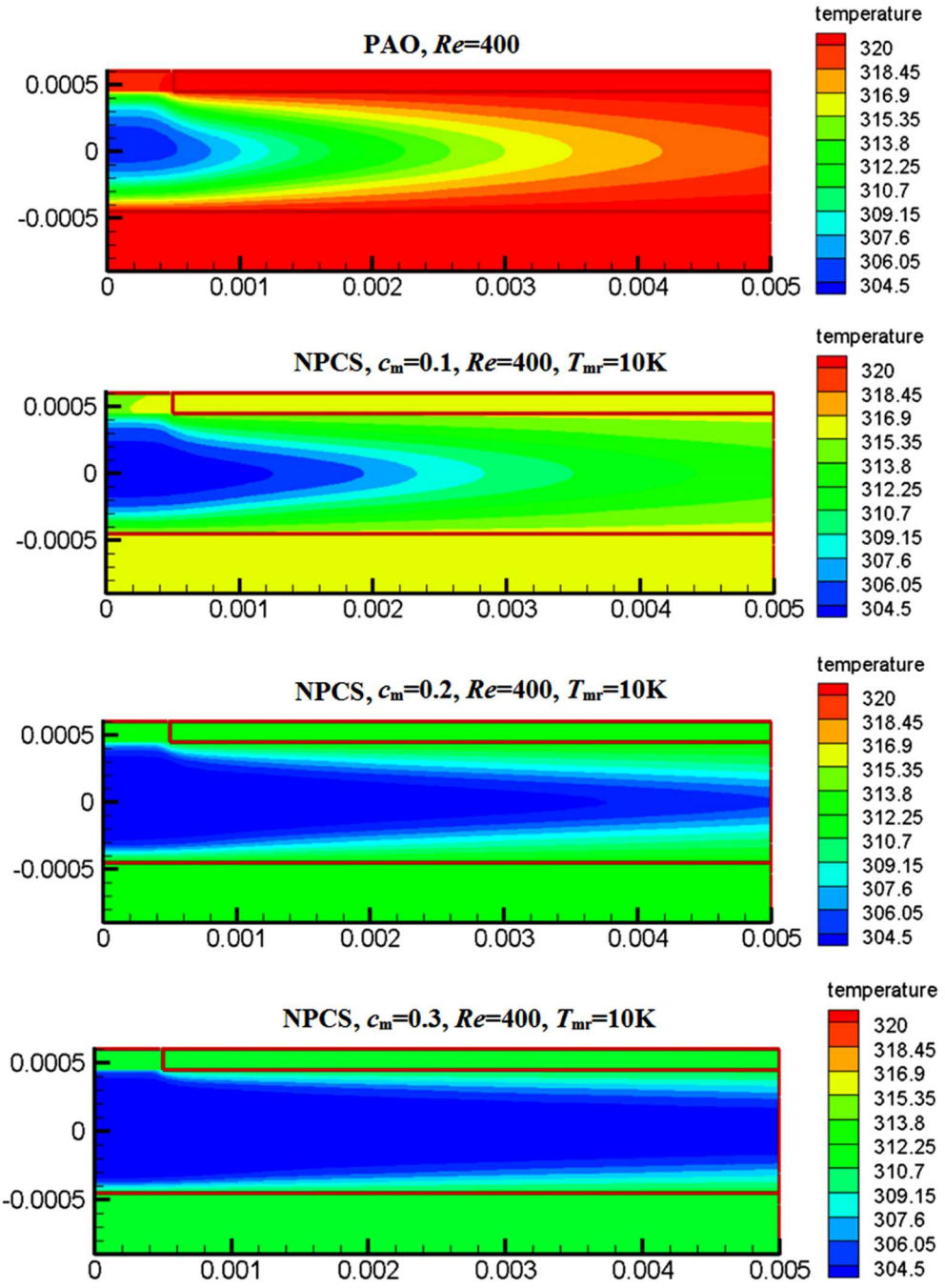

Fig. 12 Comparison of experimental data with those predicted by Eq. (29) [83]. (a) c_m = 5%, (b) c_m = 10% and (c) c_m = 15.8%.

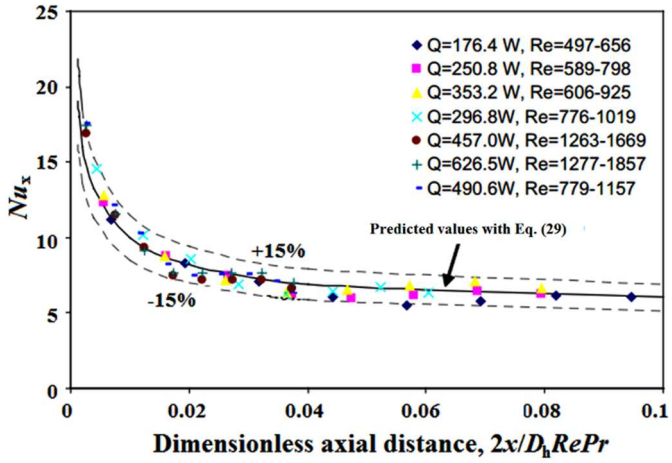

(a)

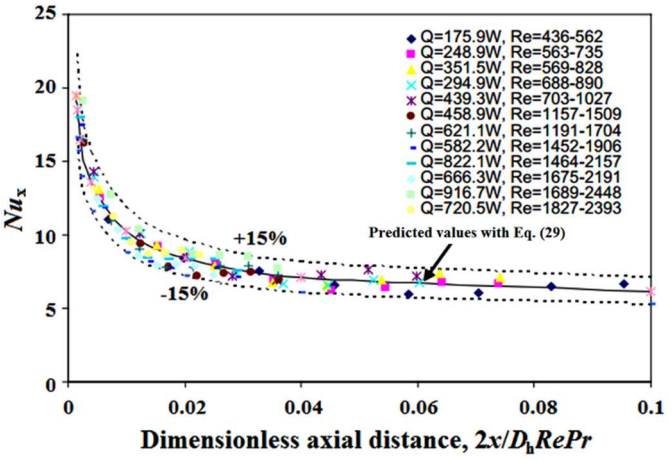

(b)

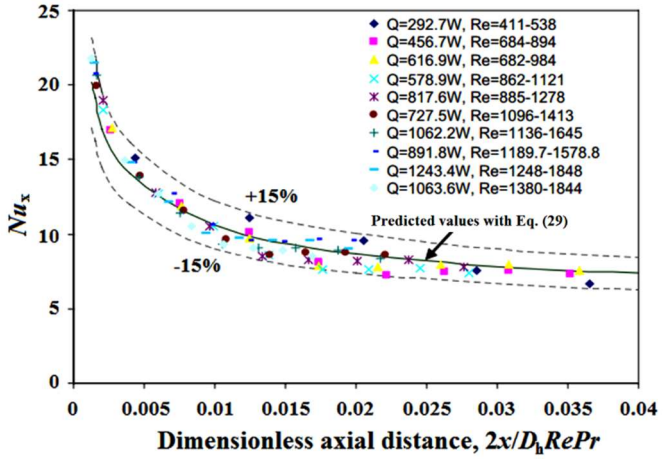

(c)